Human Molecular Genetics
hmg.oxfordjournals.org

Hum. Mol. Genet. (2015) doi: 10.1093/hmg/ddv346
First published online: August 26, 2015

Human Molecular Genetics
hmg.oxfordjournals.org

Hum. Mol. Genet. (2015) doi: 10.1093/hmg/ddv346
First published online: August 26, 2015

Synonymous variants in HTRA1 implicated in AMD susceptibility impair its capacity to regulate TGF-β signaling

Ulrike Friedrich[1,†], Shyamtanu Datta[1,†], Thomas Schubert[2,5], Karolina Plössl[1], Magdalena Schneider[3], Felix Grassmann[1], Rudolf Fuchshofer[3], Klaus-Jürgen Tiefenbach[4], Gernot Längst[2] and Bernhard H. F. Weber[1,*]

+ Author Affiliations

+ Author Affiliations

*To whom correspondence should be addressed at: Institute of Human Genetics, University of Regensburg, Franz-Josef-Strauss-Allee 11, D-93053 Regensburg, Germany. Tel: +49 941 9445400; Fax: +49 941 9445402; Email: bweb@klinik.uni-regensburg.de

† The authors wish it to be known that, in their opinion, the first two authors should be regarded as joint First Authors.

Received April 15, 2015.
Revision received July 29, 2015.
Accepted August 19, 2015.

Abstract

High-temperature requirement A1 (HTRA1) is a secreted serine protease reported to play a role in the development of several cancers and neurodegenerative diseases. Still, the mechanism underlying the disease processes largely remains undetermined. In age-related macular degeneration (AMD), a common cause of vision impairment and blindness in industrialized societies, two synonymous polymorphisms (rs1049331:C>T, and rs2293870:G>T) in exon 1 of the *HTRA1* gene were associated with a high risk to develop disease. Here, we show that the two polymorphisms result in a protein with altered thermophoretic properties upon heat-induced unfolding, trypsin accessibility and secretion behavior, suggesting unique structural features of the AMD-risk-associated HTRA1 protein. Applying MicroScale Thermophoresis and protease digestion analysis, we demonstrate direct binding and proteolysis of transforming growth factor β1 (TGF-β1) by normal HTRA1 but not the AMD-risk-associated isoform. As a consequence, both HTRA1 isoforms strongly differed in their ability to control TGF-β mediated signaling, as revealed by reporter assays targeting the TGF-β1-induced serpin peptidase inhibitor (SERPINE1, alias PAI-1) promoter. In addition, structurally altered HTRA1 led to an impaired autocrine TGF-β signaling in microglia, as measured by a strong down-regulation of downstream effectors of the TGF-β cascade

such as phosphorylated SMAD2 and PAI-1 expression. Taken together, our findings demonstrate the effects of two synonymous HTRA1 variants on protein structure and protein interaction with TGF-β1. As a consequence, this leads to an impairment of TGF-β signaling and microglial regulation. Functional implications of the altered properties on AMD pathogenesis remain to be clarified.

Introduction

The high-temperature requirement A (HTRA) family of proteins is broadly characterized by a highly conserved protease domain and one or more C-terminal PDZ protein-interaction domains (1–3). One of its members, HTRA1, is a secreted protease with an extracellular export signal, a Mac25/IGFBP domain, a Kazal-like structure, a serine protease module and a single C-terminal PDZ binding motif (3,4). Functionally, HTRA1 is thought to be involved in a number of biological processes and was reported to influence cell signaling (5–9), organization of the extracellular matrix (10–13) and skeletal development and osteogenesis (14,15).

In addition, HTRA1 was suggested to influence several disease-associated processes, particularly in CARASIL (cerebral autosomal recessive arteriopathy with subcortical infarcts and leukoencephalopathy) (16,17), osteoarthritic cartilage (10,11,18), preeclampsia (19) and choroidal neovascularization (9,13,20). HTRA1 may also mediate tumor suppressor activities (21–23), as down-regulation of the protein was observed in a variety of cancers, e.g. endometrial, ovarian or breast cancers, and melanomas (21,22,24–27). Despite its suspected role in the various diseases, the exact mechanisms of HTRA1 action are largely unknown.

DNA variants in the coding region of the *HTRA1* gene have been associated with two diseases including the autosomal dominant CARASIL (16,28–32) and the complex age-related macular degeneration (AMD) (33,34). For CARASIL, HTRA1 mutations in conserved regions of its protease domain or deleterious nonsense mutations were suggested to underlie disease pathogenesis by impairing control of HTRA1 over TGF-β-regulated pathways thus increasing levels of TGF-β in cerebral small arteries (16). In accordance with these results, HTRA1-deficient mice exhibited increased levels of phosphorylated SMAD proteins, downstream effectors of the TGF-β signaling cascade in brain tissue (9).

Several independent case–control association studies have revealed a strong association of AMD pathology with two variants located in exon 1 of the *HTRA1* gene (rs1049331:C>T, and rs2293870:G>T) (6,35–37). Although synonymous, these variants were recently shown to directly influence the ability of HTRA1 to regulate insulin-like growth factor 1 (IGF1) signaling (6). However, the binding capacity of HTRA1 for IGF1 is controversial (4).

Here, we have reanalyzed *HTRA1* variants rs1049331:C>T and rs2293870:G>T by independent methodological approaches for their effects on protein structure. In our analysis, we have also included a third variant, rs2293870:G>C, which is located at the same nucleotide position as rs2293870:G>T but is not associated with AMD disease. By MicroScale Thermophoresis (MST), we demonstrate an influence of the AMD-risk-associated polymorphisms rs1049331:C>T and rs2293870:G>T on HTRA1 protein folding but not for rs2293870:G>C. We also show that the two HTRA1 protein isoforms reveal differences in their ability to regulate TGF-β signaling. Specifically, the HTRA1 isoform translated from risk variants rs1049331:T and rs2293870:T binds less efficiently to TGF-β and is less proteolytically active. As a consequence, control over TGF-β-regulated

pathways becomes impaired although a role of these processes in AMD pathogenesis remains to be shown.

Results

Statistical evaluation of tri-allelic variant rs2293870 for AMD risk association

We evaluated the association of late-stage AMD risk with G, T and C alleles at the tri-allelic rs2293870 variant located in the exon 1 coding sequence of the HTRA1 gene. With rs2672601:A, a suitable biallelic proxy variant for the rs2293870:C allele was identified in 503 Europeans (R^2 to the C allele of rs2293870 of 0.96; 1000 Genomes project, Phase 3). We then genotyped rs2672601 (for the A allele) and rs2293870 (for the C and T allele) in 1.667 late-stage AMD cases and 1.148 AMD-free controls. Subsequently, we fitted a multivariate logistic regression model including both rs2293870 and rs2672601. In agreement with previous reports (6,35–37), we found that the T allele of rs2293870 is strongly associated with AMD [odds ratio [OR] 2.98, 95% confidence interval [CI] 2.62–3.40, $P < 1 \times 10exp-16$). On the other hand, rs2672601 (and thus the C allele of rs2293870) revealed no association with late stage AMD (OR 0.94, 95% CI 0.79–1.10, $P = 0.41$). The C allele of rs1049331 is on the same haplotype as the G and C allele of rs2293870 (non-AMD associated), and the T allele of rs1049331 is on the same haplotype as the T allele of rs2293870 (AMD associated). We observed no discordant haplotypes in 503 Europeans from the 1000G project.

Synonymous DNA variants rs1049331:C>T and rs2293870:G>T but not rs2293870:G>C in exon 1 of HTRA1 alter the conformation of the secreted protein

Three expression constructs for HTRA1 were generated including HTRA1 exon 1 variants rs1049331:C and rs2293870:G [reference haplotype (36), referred to as HTRA1:CG], the AMD-associated variants rs1049331:T and rs2293870:T (HTRA1:TT), and the non-disease-associated variants rs1049331:C and rs2293870:C (HTRA1:CC) (Fig. 1A). To assess an influence of codon usage on structural properties, we heterologously expressed the different HTRA1 variants in human Hek293 cells. Owing to the mammalian expression system and to auto-proteolytic activity of HTRA1, protein yield was low rendering several methods for structural analysis inappropriate. In addition, HTRA1 contains no tryptophan residue in its amino acid sequence, limiting the application of fluorometric methods. To assess protein folding properties of the translation products, we first applied MST, a method which determines the movement of molecules along a temperature gradient (38,39). The thermophoretic movement is very sensitive to changes of the molecular structure or conformation. To specifically detect alterations of the structure of the HTRA1 isoforms, the thermophoretic movement was determined under different temperature conditions (from 32 to 52°C in 2°C steps). The protein was fluorescently labeled at the C-terminus via its tetra-cysteine(TC) tag (40,41).

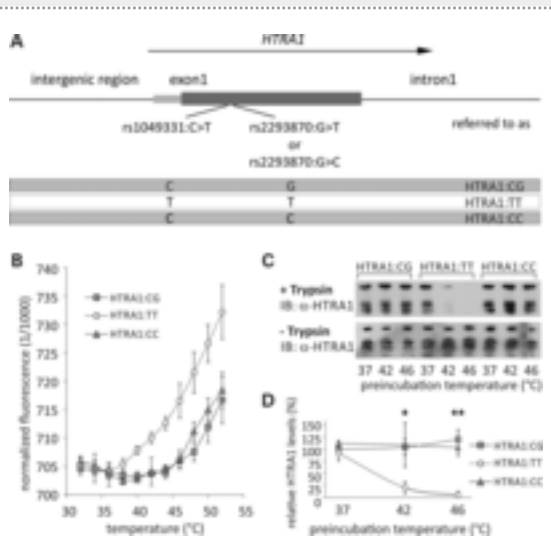

View larger version:

Figure 1.

Influence of synonymous SNPs within HTRA1 exon 1 on protein structure. (**A**) Schematic diagram of relative positions of synonymous polymorphisms used to generate expression constructs for HTRA1:CG (not associated with AMD

risk), HTRA1:TT (associated with AMD risk) and HTRA1:CC (not associated with AMD risk). (**B**) MST analysis of HTRA1:CG, HTRA1:TT and HTRA1:CC. TC-tagged HTRA1 isoforms were heterologously expressed in Hek293 cells. HTRA1 protein was determined in the supernatant via Bradford assay, adjusted to 2 µg/µl and quantified via western blot analysis with α-HTRA1 antibody. Subsequently, HTRA1 was labeled with a TC-tag-specific fluorescent dye and subjected to MST analysis. Electrophoretic mobility of the fluorescent protein was assessed at increasing temperatures (from 32 to 52°C). Supernatant of cells transfected with an empty vector was used for normalization. Data represent the mean ± standard deviation (SD) of three independent experiments. (**C**) Partial proteolysis of recombinant HTRA1:CG, HTRA1:TT and HTRA1:CC with trypsin. Strep-tagged HTRA1 isoforms were purified after heterologous expression in Hek293 cells. One microgram of purified HTRA1 was incubated for 10 min at 37, 42 and 46°C, respectively. Proteolysis was performed at 37°C for 5 min with 120 µg/ml trypsin. Samples were subjected to western blot analysis with α-HTRA1 antibodies. **(D)** Densitometric analysis of immunoblots of three independent experiments from (C). HTRA1 signals were calibrated with measurements for HTRA1:CG after preincubation at 37°C. Data represent the mean ± SD. Asterisks mark significant (*$P < 0.05$) and highly significant differences (**$P < 0.01$) between relative amounts of protein for HTRA1:CG or HTRA1:CC and HTRA1:TT.

MST analysis of the three HTRA1 constructs at different temperatures revealed a similar thermal migration behavior of the two HTRA1 isoforms HTRA1:CG and HTRA1:CC (Fig. 1B). In contrast, HTRA1:TT exhibited a significantly different thermophoretic mobility at higher temperatures (Fig. 1B) suggesting an influence of AMD-associated polymorphisms rs1049331:T and rs2293870:T on the tertiary structure of the protein.

In an independent approach, we assessed structural differences of the three protein isoforms by partial proteolysis. This assay is sensitive to minor alterations in protein structure by measuring the susceptibility of the protein substrate for proteases such as trypsin (42–45). This protease susceptibility of a protein is strongly dependent on unfolding processes and, in contrast to fluorometric detection systems, the proteases detect local and not mainly global unfolding (44). Under partial denaturing conditions, HTRA1:TT was more susceptible to trypsin digestion than HTRA1:CG or HTRA1:CC (Fig. 1C). Specifically, after preincubation at 42°C, a strong decrease of HTRA1:TT was observed, and after preincubation at 46°C, HTRA1:TT was completely digested (Fig. 1D). In contrast, no significant reduction of HTRA1:CG and HTRA1:CC, subjected to these conditions, was observed. The differences in protein levels between HTRA1:CG or HTRA1:CC and HTRA1:TT were statistically significant after preincubation at 42°C ($P < 0.05$), and highly significant after preincubation at 46°C ($P < 0.01$). Autoproteolysis of HTRA1 was negligible (Fig. 1C).

Together, the results from MST analysis and from partial proteolysis suggest that HTRA1:CG and HTRA1:CC exhibit a similar tertiary structure that is different from HTRA1:TT. With a further focus on the functional relevance of the altered structure of HTRA1:TT, following we concentrated on this variant and compared its properties with the HTRA1 isoform

translated from the reference haplotype, namely HTRA1:CG.

Delayed secretion of HTRA1 protein isoform HTRA1:TT in Hek293 cells

Secreted proteins are subjected to ER quality control, which retains and eventually degrades misfolded protein species with a high sensitivity toward minor structural alterations (46). We therefore monitored secretion of HTRA1:CG and HTRA1:TT in Hek293 cells. The supernatant and cells were collected at various time points between 0 and 24 h after transfection with expression constructs for HTRA1:CG and HTRA1:TT (Fig. 2). Western blot analysis was performed with α-HTRA1 antibody. Relative to HTRA1:CG, intracellular amounts of HTRA1:TT were increased, with a statistically significant difference at 24 h ($P < 0.05$) (Fig. 2A and B). Conversely, a reduction of HTRA1:TT protein relative to HTRA1:CG was detected in the supernatant (Fig. 2A and C). At time points 20 and 24 h, the differences in the amounts of extracellular protein of HTRA1:CG and HTRA1:TT were statistically significant ($P < 0.05$) (Fig. 2C). These data suggest a delayed secretion of HTRA1:TT relative to HTRA1:CG.

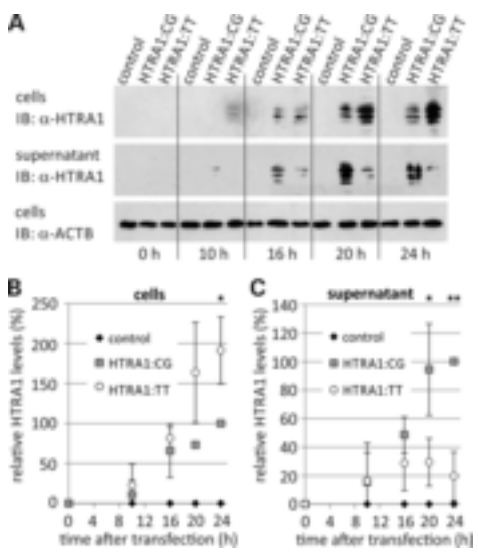

View larger version:
In this page In a new window
Download as PowerPoint Slide

Figure 2.
Influence of synonymous SNPs within HTRA1 exon 1 on protein secretion. (**A**) Immunoblot experiments to assess heterologous HTRA1 expression and secretion in Hek293 cells. After transfection of Hek293 cells with expression constructs for HTRA1:CG, HTRA1:TT or control, cells and cell culture medium (supernatant) were harvested at the indicated time points (0–24 h) and subjected to western blot analysis with α-HTRA1 antibodies. The ACTB immunoblot served as loading control. **(B)** and (**C**) Densitometric quantification of immunoblots of three independent repetitions of experiments from (A) focusing on (B) intracellular or (C) extracellular HTRA1 protein. HTRA1 signals were normalized against ACTB and calibrated against measurements for HTRA1:CG at 24 h. Data represent the mean ± SD. Asterisks mark statistically significant ($*P < 0.05$) and highly significant differences ($**P < 0.01$) between relative amount of protein for HTRA1:CG and HTRA1:TT.

HTRA1 protein isoform HTRA1:TT reveals significantly reduced TGF-β1 binding and proteolysis

Several studies demonstrated a negative, inhibiting influence of HTRA1 on TGF-β signaling, although the type of interaction between the two molecules remained controversial (5,7,9,17,47,48). To investigate the HTRA1–TGF-β interplay, we used MST analysis and measured thermophoretic mobility of HTRA1 dependent on increasing TGF-β1 concentrations. For HTRA1:CG in the presence of mature TGF-β1, we observed a typical sigmoidal binding curve with a binding affinity of 63.2 ± 8.8 nM (Fig. 3A). These results support a direct interaction between HTRA1 and mature TGF-β. We then tested TGF-β1 binding of HTRA1:TT and found that this variant failed to interact with TGF-β1 (Fig. 3A). In contrast, titration of HTRA1 with its substrate ß-casein revealed a similar sigmoidal binding curve for both HTRA1 isoforms, HTRA1:CG and HTRA1:TT. The binding affinities were 527.9 ± 96.4 nM for HTRA1:CG, and

410.3 ± 77.4 nM for HTRA1:TT, with the differences in binding affinities not being statistically significant (Fig. 3B).

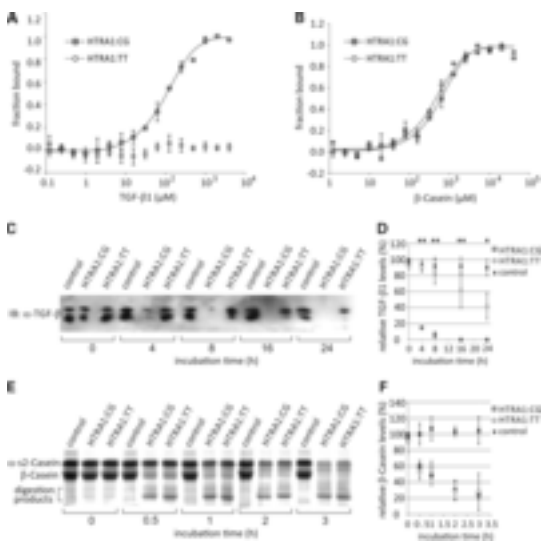

View larger version:
» In this page » In a new window
» Download as PowerPoint Slide

Figure 3.

Influence of synonymous SNPs within HTRA1 exon 1 on its substrate affinity. (**A**) HTRA1 and its interaction with TGF-β1 as measured by MST. Fluorescence-labeled HTRA1 (100 nM) was incubated with increasing concentrations of TGF-β1 (0.122–4000 nM). (**B**) HTRA1 and its interaction with β-Casein as measured by MST. Fluorescence-labeled HTRA1 (100 nM) was incubated with increasing concentrations of β-Casein (1.22–40000 nM). Protein–protein interactions for (A) and (B) where quantified by MST and binding data were plotted applying the Hill equation. The recorded fluorescence was normalized to fraction bound (0 = unbound, 1 = bound). Data represent the mean ± SD of three independent experiments. **(C)** Proteolysis of TGF-β1 by HTRA1:CG, HTRA1:TT or control. One microgram of TGF-β1 was mixed with 300 µl supernatant of transfected Hek293 cells, containing 15 ng/µl of each HTRA1 isoform, and incubated at 37°C. Samples were taken at the indicated time points. TGF-β1 proteolysis was captured via western blot analysis with α-TGF-β antibody. (**D**) Three independent experiments were performed for TGF-β1 as shown in (C) and subjected to densitometrical analysis. TGF-β1 signals were calibrated against measurements for HTRA1:CG at 0 h. Data represent the mean ± SD. Asterisks mark statistically significant (*$P < 0.05$) and highly significant differences (**$P < 0.01$) between TGF-β1 cleavage by HTRA1:CG and HTRA1:TT, respectively. (**E**) Proteolysis of β-Casein by HTRA1:CG, HTRA1:TT or control. Twenty micrograms of β-Casein were mixed with 300 µl supernatant of transfected Hek293 cells, containing 10 ng/µl of each HTRA1 isoform, and incubated at 37°C. β-Casein was visualized by Coomassie staining. (**F**). Three independent experiments were performed for β-Casein as shown in (E) and subjected to densitometrical analysis. β-Casein signals were calibrated against measurements for HTRA1:CG at 0 h. Data represent the mean ± SD.

Next, we analyzed the proteolytic capacity of HTRA1:CG and HTRA1:TT for TGF-β and β-Casein, respectively. Co-incubation of HTRA1 with mature TGF-β1 resulted in a gradual degradation of TGF-β1. However, TGF-β1 cleavage by HTRA1:TT was strongly reduced compared with HTRA1:CG (Fig. 3C). Densitometry of three independent experiments revealed that ~85% of TGF-β1 was cleaved by HTRA1:CG after 4 h, whereas only 10% of TGF-β1 cleavage was observed in the presence of HTRA1:TT (Fig. 3D). After 16 h, TGF-β1 was completely cleaved by HTRA1:CG whereas at this time point almost 60% of mature TGF-β1 was still present when incubated with HTRA1:TT (Fig. 3D). The observed differences for TGF-β1 cleavage by HTRA1:CG and HTRA1:TT were statistically highly significant ($P < 0.01$) whereas both HTRA1 isoforms exhibited similar proteolytic activities for the β-Casein substrate (Fig. 3E and F).

HTRA1 isoform HTRA1:TT exhibits a reduced capacity for TGF-β signaling inhibition

To examine whether the altered affinity of TGF-ß1 and HTRA1:TT affects TGF-β signaling, we used a reporter assay based on MLEC-PAI/Luc cells (49). These cells are stably transfected with a luciferase coding sequence under the control of the TGF-β responsive element of the *PAI-1* promoter and thus respond to stimulation by TGF-ß family members (e.g. TGF-β1) with heterologous luciferase expression (49). Addition of HTRA1:CG to MLEC-PAI/Luc cells resulted in a strong reduction of TGF-β1-activated luciferase expression (17.1 ± 3.6% luciferase activity compared with control cells). HTRA1:TT was also capable of inhibiting TGF-β1-activated luciferase expression, but only at 67.0 ± 4.5% (Fig. 4). The difference in luciferase expression between cells treated with HTRA1:CG and HTRA1:TT was statistically highly significant ($P < 0.01$).

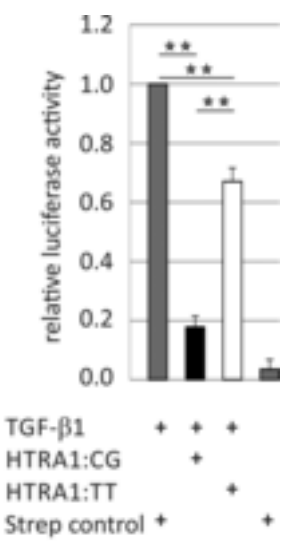

View larger version:
In this page In a new window
Download as PowerPoint Slide

Figure 4.
Effects of HTRA1:CG and HTRA1:TT on TGF-β1-induced *PAI-1* promoter activity in MLEC(PAI/Luc) cells. MLEC(PAI/Luc) cells were stimulated with 2 ng/ml TGF-β1 in the presence of 40 ng/ml HTRA1:CG or HTRA1:TT, which were purified from supernatant of Hek293 cells transfected with expression constructs for Strep-tagged HTRA1, or control protein (purified from supernatant of empty Strep-vector transfected cells). After 16 h, luciferase activity was measured in triplicate wells each in three independent experiments. Measurements for each experiment were calibrated against the control (TGF-β1 + control protein). The mean + SD for the three independent experiments is given for each treatment. Asterisks mark statistically highly significant differences (**$P < 0.01$).

HTRA1 isoform HTRA1:TT exhibits reduced control over autocrine TGF-β signaling in microglial cells

TGF-β signaling has been reported to be an important regulator of microglial activation (50–53). Specifically, extracellular binding of TGF-β family members by TGF-β receptors leads to phosphorylation of SMAD proteins (54–56). We therefore analyzed the influence of HTRA1:CG and HTRA1:TT on the phosphorylation of SMAD2 in BV-2 cells (Fig. 5). Immunocytochemistry with control cells showed a strong immunoreactivity for phosphorylated SMAD2 (pSMAD2) within BV-2 cells, indicating an activated TGF-β signaling pathway by endogenously synthesized and secreted TGF-β proteins (Fig. 5A, left), in full agreement with data on autocrine TGF-β expression and signaling in microglial cells (57). BV-2 cells treated with HTRA1:CG exhibited a significantly reduced signal intensity of pSMAD2 indicating an inhibiting effect of HTRA1:CG upon TGF-β signaling (Fig. 5A, middle). In contrast, staining for pSMAD2 in BV-2 cells treated with HTRA1:TT had a similar intensity as in the control experiment (Fig. 5A, right). To quantify the effects of HTRA1 isoforms on SMAD phosphorylation, we performed western blot analyses and densitometry (Fig. 5B and C). The data show that SMAD2 phosphorylation

is almost completely absent in BV-2 cells treated with HTRA1:CG whereas HTRA1:TT reduced measurable pSMAD2 levels to 71.9 ± 2.5% compared with control (Fig. 5B and C). While the amounts in SMAD2 protein were comparable, the observed differences in phosphorylated pSMAD2 were statistically highly significant ($P < 0.01$) (Fig. 5C).

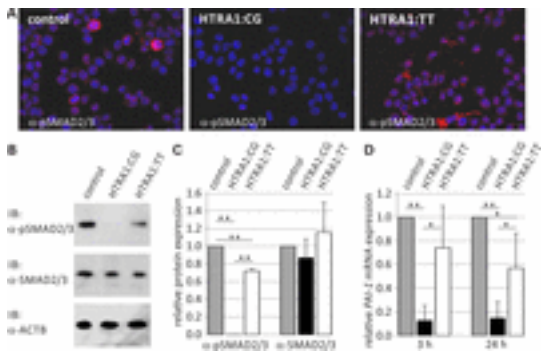

View larger version:
In this page In a new window
Download as PowerPoint Slide

Figure 5.

Effect of HTRA1:CG and HTRA1:TT on autocrine TGF-β signaling in BV-2 cells. (**A**) Activation of the SMAD cascade. BV-2 cells were treated for 2 h with HTRA1:CG, HTRA1:TT or control protein, the latter purified from supernatant of empty Strep-vector transfected cells. Subsequently, the cells were subjected to immunocytochemistry with antibodies against pSMAD2. (**B**) Alternatively, cells from (A) were analyzed by western blot analysis with antibodies against pSMAD2, the SMAD2 protein or ACTB as a control. (**C**) Densitometric quantification of immunoblots from (B) with three independent experiments. Signals for pSMAD2 and SMAD2 were normalized against ACTB and calibrated against the control. Data represent the mean ± SD. **(D)** *PAI-1* expression in BV-2 cells. BV-2 cells were treated for 3 and 24 h with recombinant HTRA1:CG, HTRA1:TT or control protein. *PAI-1* mRNA expression was determined via quantitative real-time RT-PCR. Experiments were performed in triplicates in four independent experiments, respectively. Results were normalized to *GNB2L* transcript levels and calibrated with the control at 3 and 24 h, respectively. The mean + SD for the four independent experiments is given. Asterisks mark statistically significant (*$P < 0.05$) and highly significant differences (**$P < 0.01$).

Upon TGF-β stimulation, phosphorylated SMAD2 and SMAD3 form a complex with SMAD4, which is then translocated into the nucleus and stimulates expression of TGF-β response genes (54-56). After treating BV-2 cells with HTRA1:CG and HTRA1:TT for 3 and 24 h, we monitored the expression of *PAI-1*, a prominent target gene of TGF-β signaling (58-60) (Fig. 5D). Upon quantitative RT-PCR, a strong down-regulation of *PAI-1* mRNA expression was noted in BV-2 cells treated with HTRA1:CG when compared with control cells (12.5 ± 12.9% after 3 h; 14.5 ± 13.9% after 24 h). In contrast, a less prominent decrease of *PAI-1* transcripts was found after treatment with HTRA1:TT (74.0 ± 35.5% after 3 h; 56.8 ± 29.6% after 24 h, compared with control cells). The difference in *PAI-1* expression following treatment with HTRA1:CG or HTRA1 TT was statistically significant ($P < 0.05$).

Discussion

The present study focused on the impact of three synonymous SNPs (rs1049331:C>T, rs2293870:G>T and rs2293870:G>C) on HTRA1 structure and function. We first re-analyzed AMD association of these three SNPs located in coding exon 1 of the *HTRA1* gene in nearly 3000 individuals with and without AMD disease. In agreement with earlier reports (6,35-37), we show that the rs2293870:T allele is indeed highly associated with AMD whereas genotyping a perfect proxy for the

rs2293870:C allele (rs2672601:A) revealed no association with disease risk. We now provide evidence that the rs1049331:T/rs2293870:T haplotype (HTRA1:TT) significantly alters HTRA1 folding and the ability of the protein to bind TGF-β1. The third SNP (rs2293870:G>C) despite affecting the identical nucleotide position as rs2293870:G>T revealed functional features comparable with the reference sequence (rs1049331:C, rs2293870:G or HTRA1:CG).

In recent years, the influence of synonymous, silent mutations on protein folding and function has attracted increasing attention (61). These alterations although not associated with changes in amino acid composition of the protein were reported to cause mRNA instability, exon skipping or alterations in co-translational protein folding (43,62–70). As a consequence, synonymous alterations in protein-coding sequences may causally be involved in human pathologies. For example, synonymous changes in the multidrug resistance 1 (*MDR1*) gene were shown to cause an altered drug and inhibitor interaction leading to major changes in protein stability and transporter specificity (43,71).

Interestingly, in the present study, thermophoretic movement and trypsin accessibility of HTRA1 were significantly altered only for the protein isoform encoded by the transcript harboring the synonymous variants rs1049331:T and rs2293870:T (HTRA1:TT), but not for the two other isoforms, harboring rs1049331:C and rs2293870:G (HTRA1:CG), or rs1049331:C and rs2293870:C (HTRA1:CC). Also, we provide evidence for a decreased secretion of the AMD-associated HTRA1 variant over the reference isoform. The impact of the synonymous nucleotide changes at HTRA1:CG, HTRA1:TT and HTRA1:CC on its protein structures remains to be determined. They localize to the N-terminal domain of HTRA1, known as the IGFBP-like module, which exhibits a similar fold as the N-terminal lobe of the IGF-binding protein (4). This domain apparently has no influence on folding or protease activity of the HTRA1 C-terminus (4) but could mediate protein-protein interactions (6). This suggests that a structural alteration of this domain could alter substrate binding capacities of HTRA1.

Our results are in full agreement with findings first reported by Jacobo and colleagues (6). In their work, the authors observed a decreased translation rate of the isoform HTRA1:TT which they ascribed to differential codon usage (6). They also reported differential susceptibilities of this variant toward proteolysis, an anti-HTRA1 antibody and IGF-1 interaction. However, the interaction between HTRA1 and IGF-1 is challenged by findings from Eigenbrot and colleagues (4) who failed to obtain evidence for a binding of IGF-I, IGF-II or insulin binding activity for the N-domain of HTRA1. This is further supported by a biosensor binding study which found no appreciable Mac-25 interaction of HTRA1 with IGF-I or IGF-II (72).

We therefore focused on the widely reported influence of HTRA1 on TGF-β signaling (5,7,9,17,47,48). Although generally accepted, the precise mechanism of HTRA1 interference with this pathway is still contested. Initially, HTRA1 was shown to bind to but not cleave mature TGF-β proteins (7) whereas other studies observed direct proteolysis of mature TGF- β family members by HTRA1 (9,47). Afterward, the latter findings were refuted by Shiga and colleagues, who described proteolysis by HTRA1 only for the intracellular pre-form of TGF-β (17). Similarly, Graham and colleagues also could not find an interaction of HTRA1 and TGF-β but instead described cleavage of TGF-β receptors by HTRA1 (5). Applying MST and TGF-β digestion analyses, we provide evidence for a direct proteolytic activity of isoform HTRA1:CG toward mature TGF-β1 in

agreement with earlier reports (9,47). Nevertheless, we cannot exclude other so far unknown sites of interaction at which HTRA1 antagonizes the TGF-β pathway.

Interestingly, the MST data presented here revealed no stable interaction between HTRA1:TT and TGF-β1, whereas the TGF-β1 *in vitro* digestion assay suggested a strongly decreased turnover rate of TGF-β1 by HTRA1:TT compared with HTRA1:CG. The apparent discrepancy raises the question why there is still an interaction of TGF-β1 and HTRA1 in the proteolysis assay, whereas at the same time, no interaction of the two proteins is apparent in the MST assay. We hypothesize that MST measures a stable interaction between HTRA1 and TGF-β1, resulting in a binding constant whereas the proteolytic assay measures enzyme kinetics over a longer period of time. A stable interaction between protease and substrate is not necessary for proteolytic cleavage, as described e.g. for rhomboid proteases (73). These proteases displayed no physiological affinity for their substrates. Instead, an approximate 10 000-fold difference in proteolytic efficiency with substrate mutants and diverse rhomboid proteases were reflected in kcat values alone.

The reduced proteolytic capacity of HTRA1:TT for TGF-β1 severely affected the regulation of TGF-β signaling by HTRA1, as observed in reporter assays assessing the *PAI-1* promoter, a prominent target of the TGF-β cascade. In agreement with this, Hara and colleagues (16) reported similar consequences owing to CARASIL-associated *HTRA1* variants. Specifically, two nonsense mutations and one missense mutation in *HTRA1* resulted in protein products that failed to repress signaling by the TGF-β family (16). As increased TGF-β levels were observed in cerebral arteries of CARASIL patients, the authors concluded that HTRA1 contributes to the pathogenic processes of CARASIL via its control of TGF-β signaling. In this context, it is interesting to note that increased TGF-β levels are also observed in AMD patients (74,75) and aberrant TGF-β signaling was connected to AMD-related phenotypes in mice (9,76,77) and RPE cells (77–80). This and our findings could imply a role for HTRA1 in AMD pathogenesis via its regulation of the TGF-β pathway.

We also demonstrated control of HTRA1 over TGF-β regulation in cultured microglial cells. Microglia are the major resident inflammatory cells of the central nervous system and obtain key functions of immune surveillance and tissue repair (81–83). Thus, this cell type is deeply involved in the pathogenic processes of various neurodegenerative diseases like Parkinson's disease (84), Alzheimer's disease (85–89), inherited retinopathies (90) or AMD (91–95). In addition, activation and differentiation of microglia is strongly regulated by TGF-β signaling (96–99). We now showed that pSMAD2 and *PAI-1* expression, both markers for an activated TGF-β signaling (54–56,58–60), were significantly lower in microglial (BV-2) cells treated with HTRA1. Thus, our data further provide evidence for a role of HTRA1 in the differentiation and activation of microglia, and therefore likely in the pathogenesis of neurodegenerative disease. Of note, the inhibitory effect of HTRA1:TT on microglial TGF-β signaling was weaker compared with the reference HTRA1 isoform, HTRA1:CG.

Taken together, our data show that HTRA1 is an important regulator of TGF-β signaling by direct interaction with and cleavage of TGF-β. AMD-associated polymorphisms in HTRA1 (rs1049331:T/rs2293870:T) result in delayed protein secretion, reduced TGF-β1 affinity and decreased capacity to control TGF-β signaling and autocrine TGF-β regulation in microglia. One might therefore be tempted to speculate about a functional contribution of AMD-associated polymorphisms in HTRA1 to AMD

pathogenesis. However, it has also been shown that gene expression of *HTRA1* is highly heterogeneous among different individuals, independent of their *HTRA1* genotype (100), with expression levels of HTRA1 varying up to 20-fold. In principle, this questions an involvement of reduced HTRA1 activity on AMD development. Moreover, owing to high LD within the chromosomal *HTRA1* gene locus, a number of additional polymorphisms reveal an equally strong association with AMD extending to and encompassing variants at the neighboring *ARMS2* gene. The final decision which gene, *HTRA1* or *ARMS2*, is causally involved in AMD pathogenesis requires further scrutiny and specifically needs the understanding of functional aspects of the as of yet unknown ARMS2 protein.

Materials and Methods

Genotyping the C-allele of rs2293870 and statistical evaluation

Owing to the tri-allelic nature of the variant rs2293870, direct genotyping is challenging. We therefore searched for a suitable biallelic proxy variant for the C-allele of rs2293870 in 503 European individuals from the 1000 Genomes project [allele frequency in Europeans: 0.16, Phase 3, accessed July 2015 (101)]. The biallelic variation rs2672601 (G>A, allele frequency of A in Europeans: 0.16) is in high linkage disequilibrium with rs2293870 ($R^2 > 0.96$, $D' = 1$), and the A allele of this variation was used as a surrogate for rs2293870:C. We genotyped a total of 2.815 individuals as previously described (102) and coded the genotype at rs2672601 as the number of A alleles (0, 1 or 2) and at rs2293870 as the number of T (risk associated) alleles (0, 1 or 2). Multivariate logistic regression implemented in *R* (103) was used to evaluate the association of the A allele of rs2672601 and T allele of rs2293870 with AMD risk.

Expression cloning

The coding sequences of three *HTRA1* haplotypes were heterologously expressed in Hek2893 cells. These included the most frequent *HTRA1* haplotype (HTRA1:CG), as well as two less common HTRA1 haplotypes (HTRA1:TT and HTRA1:CC) (Fig. 1A). After genotyping, the respective coding sequences were amplified from cDNA of retinal tissue as described (100).

For MST analyses, the three *HTRA1* haplotypes were each tagged with a C-terminal tetra-cysteine (TC) tag [5′ TGT TGT CCT GGC TGT TGC 3′] and cloned into the *NotI/XhoI* site of the pCEP4 vector (Invitrogen, Carlsbad, CA). Oligonucleotide primers for amplification were designed to contain a *NotI* site 5′ of the *HTRA1* translational start site (HTRA1-NotI-F, 5′ GCG GCC GCG CGC ACT CGC ACC CGC T 3′) and a TC tag followed by an *XhoI* site at the 3′-end of the *HTRA1*-coding sequence (HTRA1-TC-XhoI-R, 5′ GCA ACA GCC AGG ACA ACA TGG GTC AAT TTC TTC GGG AAT CAC TGT GAT CTC GAG CTA GCA ACA GCC AGG ACA ACA TGG GTC AAT TTC TT 3′).

For purification, coding sequences of HTRA1:CG, HTRA1:TT and HTRA1-CC were cloned into the *BamHI/XhoI* site of the pEXPR-IBA103 vector (IBA Life Sciences) fusing the insert to a Twin-Strep-Tag. Primers for amplification were designed to contain a *BamHI* site 5′ of the *HTRA1* start codon (HTRA1-ORF-BamHI-F, 5′ GGA TCC ATG CAG ATC CCG CGC GCC GCT CTT CTC C 3′) and a *XhoI* site at the 3′-end of the *HTRA1*-coding sequence (HTRA1-ORF_w/o_stop-XhoI-R, 5′ CTC GAG TGG GTC AAT TTC TTC GGG AAT CAC T 3′).

To analyze secretion, coding sequences of HTRA1:CG and HTRA1:TT were cloned into the *NotI/XhoI* site of the pCEP4 vector (Invitrogen). Primers for amplification were designed to contain a *NotI* site 5′ of the *HTRA1*

translational start site (HTRA1-NotI-F, 5′ GCG GCC GCG CGC ACT CGC ACC CGC T 3′) and a *XhoI* site at the 3′-end of the *HTRA1*-coding sequence (Htra1-ORF-XhoI-R, 5′ CTC GAG CTA TGG GTC AAT TTC TTC GGG AAT CAC T 3′).

Cell culture

Hek293-EBNA cells (Invitrogen) and MLEC-PAI/Luc cells (ATCC, Manassas, VA) were maintained in DMEM high glucose medium containing 10% FCS, 100 U/ml penicillin/streptomycin and 500 µg/ml G418 (Gibco Life Technologies). BV-2 cells were cultivated in RPMI/5% FCS supplemented with 100 U/ml penicillin/streptomycin and 195 nM β-mercaptoethanol (Gibco Life Technologies) as described by Ebert and colleagues (104). Cell lines were grown in a 37°C incubator with a 5% CO_2 environment.

Expression of HTRA1 haplotypes in Hek293-EBNA cells

Hek293-Ebna cells were seeded overnight in 10-cm cell culture dishes. At 70% confluence, the cells were transfected with 10 µg of the respective HTRA1 expression constructs and 30 µl TransIT-LT1 Transfection Reagent (Mirus Bio LLC, Madison, WI) following the manufacturer's instructions. Twenty-four hours after transfection, cell culture medium was changed to serum-free medium.

For MST analysis, the supernatant of Hek293-Ebna cells transfected with TC-tagged HTRA1 expression constructs was harvested 24 h after medium change and concentrated with Amicon Ultra 4-ml Filters (Merck Millipore, Billerica, MA). Protein concentration was determined via Bio-Rad protein assay (Bio-Rad laboratories, Hercules, CA), adjusted to 2 µg/µl and quality controlled via western blot analysis via α-HTRA1 antibody detection (see below). For purification of Strep-tagged HTRA1 proteins, the supernatant of Hek293-Ebna cells transfected with Strep-tagged HTRA1 expression constructs was harvested after 48 h.

To analyze HTRA1 secretion from Hek293-Ebna cells, cells were seeded overnight into six-well plates using Opti-MEM I Reduced Serum Medium (Gibco Life Technologies). At 70% confluence, the cells were transfected with 2.5 µg of the untagged *HTRA1* expression constructs (HTRA1:CG, HTRA1:TT or empty vector) and 7.5 µl TransIT-LT1 Transfection Reagent (Mirus Bio LLC) following the manufacturer's instructions. Supernatant and cells were harvested 10, 16, 20 and 24 h after transfection.

Microscale thermophoresis

For MST analysis, TC-tagged HTRA1 proteins (2 µg/µl each) were labeled in cell culture medium with 5 µM FlAsH-EDT2 fluorescence labeling reagent (Invitrogen). The temperature-dependent structural assays were performed as biological triplicates at 15% LED (light-emitting diode) power and 50% MST power in standard capillaries in a Monolith NT.115 (NanoTemper Technologies, Munich, Germany) with varied temperatures (32–52°C). The recorded MST signal of each protein was normalized to the same baseline fluorescence and plotted against the temperature into one graph using KaleidaGraph 4.1.

MST-binding experiments were carried out with 100 nM labeled HTRA1 in supernatant with varied concentrations of recombinant TGF-β1 (PeproTech, Hamburg, Germany) and β-casein from bovine milk (Sigma-Aldrich, St. Louis, MO) at 50% MST power, 20% LED power in standard capillaries on a Monolith NT.115 at 25°C. The recorded MST signals are normalized to the fraction of the protein bound (0 = unbound, 1 = bound) and processed with KaleidaGraph 4.1 software. The data were fitted with the help of the quadratic fitting formula (Kd formula) derived from the law of mass action. Each binding experiment was done with biological triplicates.

Twin-Strep-tag protein purification

The purification of Strep-tagged HTRA1 protein was done with the Twin-Strep-tag purification Kit (IBA Life Sciences) from supernatant of transfected Hek293-Ebna cells according to the manufacturer's protocol.

Sodium dodecyl sulfate–polyacrylamide gel electrophoresis, western blot analysis and Coomassie staining

For sodium dodecyl sulfate--polyacrylamide gel electrophoresis (SDS-PAGE), Laemmli Buffer (105) was added to the samples and the proteins were separated on 15% gels. For western blotting, proteins were transferred to polyvinylidene difluoride membranes (Immobilon, Milipore, Schwalbach, Germany). Membranes were blocked in phosphate-buffered saline (PBS, 2.7 mm KCl, 140 mM NaCl, 10 mM phosphate, pH 7.4) containing 0.05% Tween-20 (PBST) containing 3.5% nonfat dry milk (Carl Roth GmbH &Co. KG, Karlsruhe, Germany), or BSA (AppliChem GmbH, Darmstadt, Germany, only for TGF-β1 detection) for 1 h. Subsequently, membranes were incubated with primary antibodies in PBS overnight at 4°C. Primary antibodies were obtained commercially as follows: HTRA1 (ab65902; rabbit polyclonal, application as a 1:2000 dilution, Abcam, Cambridge, UK), phospho-SMAD2 (Ser465/467) (rabbit polyclonal, 1:1000, Cell Signaling Technology, Beverly, MA), SMAD2 (rabbit monoclonal, 1:1000, Cell Signaling Technology), TGF-β1 (sc-146; rabbit polyclonal, 1:10 000, Santa Cruz Biotechnology, Inc., TX) and ACTB (anti β-actin, mouse monoclonal, 1:10 000, Sigma-Aldrich). After incubation with goat anti-rabbit or goat anti-mouse IgG horseradish peroxidase (HRP)-linked antibodies (1:10 000, Calbiochem, Merck Chemicals GmbH, Schwalbach, Germany), western blots were visualized with SuperSignal West PICO Chemiluminescent Substrate (Thermo Scientific, Rockford, IL). For Coomassie staining, SDS gels were incubated in staining solution [0.1% Brilliant Blue R 250 (Sigma-Aldrich) in 10% Methanol, and 30% acidic acid] and destained in 10% Methanol and 30% acidic acid. Densitometry was performed with Total lab TL100 software (Nonlinear Dynamics, Durham, NC).

Partial proteolysis assay

One microgram of purified Strep-tagged HTRA1 (HTRA1:CG, HTRA1:TT or HTRA1-CC) in 150 mM Tris-HCl (pH 8.0), 100 mM NaCl (TBS), was preincubated at 37, 42 or 46°C for 10 min before exposure to 120 µg/ml TPCK-trypsin (Sigma-Aldrich) at 37°C for 5 min. The reaction was stopped by adding 5× Laemmli Buffer and boiling the sample for 10 min at 90°C. Subsequently, the samples were subjected to western blot analysis with α-HTRA1 antibody.

Casein *in vitro* digestion

Bioactivity of HTRA1 protein from supernatant or purified HTRA1 was tested in *in vitro* ß-casein digestions. Twenty-micrograms of ß-casein from bovine milk (Calbiochem) in 100 µl 50 mM Tris-HCl pH 7.6, 5 mM $CaCl_2$ and 150 mM NaCl was mixed with 300 µl supernatant of transfected Hek293-Ebna cells or with purified HTRA1 protein (50 ng/µl in 100 µl 50 mM Tris-HCl pH 7.6, 5 mM $CaCl_2$ and 150 mM NaCl). Samples were incubated at 37°C over a period of 3 h. After half an hour, 1, 2 and 3 h, 50 µl aliquots were taken and the reaction was stopped by adding 5× Laemmli Buffer and boiling the sample for 10 min at 90°C. Samples were resolved by SDS-PAGE and stained with Coomassie.

To compare ß-Casein cleavage catalyzed by HTRA1:CG and HTRA1:TT, ß-Casein was incubated with 300 µl serum-free medium of Hek293-Ebna cells transfected with expression constructs for HTRA1:CG and HTRA1:TT, respectively. The HTRA1 concentration was determined with Bio-Rad

protein assay (Bio-Rad laboratories), adjusted to 15 ng/µl and controlled via western blot analysis with α-HTRA1 antibody.

TGF-β1 *in vitro* digestion

One microgram of recombinant TGF-β1 (PeproTech) in 100 µl 50 mM Tris-HCl pH 7.6, 5 mM $CaCl_2$ and 150 mM NaCl was incubated with 300 µl serum-free medium of Hek293-Ebna cells transfected with the expression constructs for HTRA1:CG and HTRA1:TT, respectively. The HTRA1 concentration was determined by Bio-Rad protein assay (Bio-Rad laboratories), adjusted to 15 ng/µl and controlled via western blot analysis with α-HTRA1 antibody. Aliquots were collected at 0, 4, 8, 16 and 24 h and boiled with Laemmli Buffer to stop the reaction. Samples were subjected to western blot analysis with α-TGF-β1.

Reporter assay

MLEC-PAI/Luc cells were seeded into 96-well plates at a density of 1.5×10^4 cells per well and treated with 2 ng/ml of recombinant TGF-β1 (PeproTech) in combination with 40 ng/ml of purified HTRA1 (Strep-tagged HTRA1:CG or HTRA1:TT) or eluate of empty vector. After 16 h, luciferase activity was determined as described previously (100).

Analysis of TGF-β signaling in BV-2 cells

BV-2 cells were seeded in 12-well cell culture plates at a density of 1.5×10^5 (for immunocytochemistry) and in 6-well cell culture plates at a density of 3×10^5 (for western blot analysis). To induce autocrine TGF-β signaling, cells were serum-starved for 2 h as described by Spittau and colleagues in 2013 (57) and then incubated with 40 ng/ml of Strep-tagged HTRA1 (HTRA1:CG or HTRA1:TT), or empty vector eluate for 2 h (SMAD signaling), or 3 and 24 h (*PAI-1* expression).

Immunocytochemistry

Immunocytochemistry with α-phospho-SMAD2 (1:100, Cell Signaling Technology) and Cy3-conjugated rabbit secondary antibody (1:2000, Jackson ImmunoResearch, West Grove, NJ) was performed as described by Karlstetter and colleagues (106).

Quantitative real-time RT–PCR

Quantitative real-time RT-PCR was performed and analyzed as described (100). The following primers were used to detect transcripts of *PAI-1* (mmPAI-1-FWD: 5′ AGA CAA TGG AAG GGC AAC AT 3′ and mmPAI-1-REV: 5′ TCT GAG GTC CAC TTC AGT CTC C 3′) and GNB2L (mmGNB2L-FWD: 5′ TCT GCA AGT ACA CGG TCC AG 3′ and mmGNB2L-REV: 5′ GAG ACG ATG ATA GGG TTG CTG 3′). *PAI-1* expression was normalized to *GNBL2*.

Funding

This work was supported in part by grants from the Deutsche Forschungsgemeinschaft (DFG) (WE1259/19-1 and WE1259/19-2 to B.H.F.W.).

Acknowledgements

We thank Thomas Langmann and Marcus Karlstetter (Laboratory for Experimental Immunology of the Eye, Department of Ophthalmology, University of Cologne, Germany) for providing BV-2 cells. We also thank Raphael Lange (Institute of Human Genetics, University of Regensburg, Germany) for excellent technical assistance.

Conflict of Interest statement: None declared.

References

1. Malet H., Canellas F., Sawa J., Yan J., Thalassinos K., Ehrmann M., Clausen T., Saibil H.R. (2012) Newly folded substrates inside the molecular cage of the HtrA chaperone DegQ. Nat. Struct. Mol. Biol., 19, 152–157.
»Penn Text »CrossRef »Medline

2. Singh N., Kuppili R.R., Bose K. (2011) The structural basis of mode of activation and functional diversity: a case study with HtrA family of serine proteases. Arch. Biochem. Biophys., 516, 85–96.
»Penn Text »CrossRef »Medline »Web of Science

3. Zumbrunn J., Trueb B. (1996) Primary structure of a putative serine protease specific for IGF-binding proteins. FEBS Lett., 398, 187–192.
»Penn Text »CrossRef »Medline »Web of Science

4. Eigenbrot C., Ultsch M., Lipari M.T., Moran P., Lin S.J., Ganesan R., Quan C., Tom J., Sandoval W., van Lookeren Campagne M., et al. (2012) Structural and functional analysis of HtrA1 and its subdomains. Structure, 20, 1040–1050.
»Penn Text »CrossRef »Medline

5. Graham J.R., Chamberland A., Lin Q., Li X.J., Dai D., Zeng W., Ryan M.S., Rivera-Bermudez M.A., Flannery C.R., Yang Z. (2013) Serine protease HTRA1 antagonizes transforming growth factor-beta signaling by cleaving its receptors and loss of HTRA1 in vivo enhances bone formation. PloS one, 8, e74094.
»Penn Text »CrossRef »Medline

6. Jacobo S.M., Deangelis M.M., Kim L.K., Kazlauskas A. (2013) Age-related macular degeneration-associated silent polymorphisms in HtrA1 impair its ability to antagonize insulin-like growth factor 1. Mol. Cell. Biol., 33, 1976–1990.
»Abstract/FREE Full Text

7. Oka C., Tsujimoto R., Kajikawa M., Koshiba-Takeuchi K., Ina J., Yano M., Tsuchiya A., Ueta Y., Soma A., Kanda H., et al. (2004) HtrA1 serine protease inhibits signaling mediated by Tgfbeta family proteins. Development, 131, 1041–1053.
»Abstract/FREE Full Text

8. Supanji XXX, Shimomachi M., Hasan M.Z., Kawaichi M., Oka C. (2013) HtrA1 is induced by oxidative stress and enhances cell senescence through p38 MAPK pathway. Exp. Eye Res., 112, 79–92.
»Penn Text »CrossRef »Medline

9. Zhang L., Lim S.L., Du H., Zhang M., Kozak I., Hannum G., Wang X., Ouyang H., Hughes G., Zhao J., et al. (2012) High temperature requirement factor A1 (HTRA1) gene regulates angiogenesis through transforming growth factor-beta family member growth differentiation factor 6. J. Biol. Chem., 287, 1520–1526.
»Abstract/FREE Full Text

10. Chamberland A., Wang E., Jones A.R., Collins-Racie L.A., LaVallie E.R., Huang Y., Liu L., Morris E.A., Flannery C.R., Yang Z. (2009) Identification of a novel HtrA1-susceptible cleavage site in human aggrecan: evidence for the involvement of HtrA1 in aggrecan proteolysis in vivo. J. Biol. Chem., 284, 27352–27359.
»Abstract/FREE Full Text

11. Grau S., Richards P.J., Kerr B., Hughes C., Caterson B., Williams A.S., Junker U., Jones S.A., Clausen T., Ehrmann M. (2006) The role of human HtrA1 in arthritic disease. J. Biol. Chem., 281, 6124–6129.
»Abstract/FREE Full Text

12. Mauney J., Olsen B.R., Volloch V. (2010) Matrix remodeling as stem cell recruitment event: a novel in vitro model for homing of human bone marrow stromal cells to the site of injury shows crucial role of extracellular collagen matrix. Matrix Biol., 29, 657–663.
»Penn Text »CrossRef »Medline

13. Vierkotten S., Muether P.S., Fauser S. (2011) Overexpression of HTRA1 leads to ultrastructural changes in the elastic layer of Bruch's membrane via cleavage of extracellular matrix components. PloS one, 6, e22959.
»Penn Text »CrossRef »Medline

14. Hadfield K.D., Rock C.F., Inkson C.A., Dallas S.L., Sudre L., Wallis G.A., Boot-Handford R.P., Canfield A.E. (2008) HtrA1 inhibits mineral deposition by osteoblasts: requirement for the protease and PDZ domains. J. Biol. Chem., 283, 5928–5938.
»Abstract/FREE Full Text

15. Tsuchiya A., Yano M., Tocharus J., Kojima H., Fukumoto M., Kawaichi M., Oka C. (2005) Expression of mouse HtrA1 serine protease in normal bone and cartilage and its upregulation in joint cartilage damaged by experimental arthritis. Bone, 37, 323–336.
»Penn Text »CrossRef »Medline »Web of Science

16. Hara K., Shiga A., Fukutake T., Nozaki H., Miyashita A., Yokoseki A., Kawata H., Koyama A., Arima K., Takahashi T., et al. (2009) Association of HTRA1 mutations and familial ischemic cerebral small-vessel disease. N. Engl. J. Med., 360, 1729–1739.
»Penn Text »CrossRef »Medline »Web of Science

17. Shiga A., Nozaki H., Yokoseki A., Nihonmatsu M., Kawata H., Kato T., Koyama A., Arima K., Ikeda M., Katada S., et al. (2011) Cerebral small-vessel disease protein HTRA1 controls the amount of TGF-beta1 via cleavage of proTGF-beta1. Hum. Mol. Genet., 20, 1800–1810.
»Abstract/FREE Full Text

18. Polur I., Lee P.L., Servais J.M., Xu L., Li Y. (2010) Role of HTRA1, a serine protease, in the progression of articular cartilage degeneration. Histol. Histopathol., 25, 599–608.
»Penn Text »Medline »Web of Science

19. Ajavi E., Kongoasa N., Caffey T., Asmann Y.W., Watson W.J., Baldi A., Lala P., Shridhar V., Brost B., Chien J. (2008) Elevated expression of serine protease HtrA1 in preeclampsia and its role in trophoblast cell migration and invasion. Am J. Obstet. Gynecol., 199, 557.e1–e10.
»Penn Text »Medline

20. Nakayama M., Ieiima D., Akahori M., Kamei J., Goto A., Iwata T. (2014) Overexpression of Htra1 and exposure to mainstream cigarette smoke leads to choroidal neovascularization and subretinal deposits in aged mice. Invest. Ophthalmol. Vis. Sci., 55, 6514–6533.
»Abstract/FREE Full Text

21. Baldi A., De Luca A., Morini M., Battista T., Felsani A., Baldi F., Catricala C., Amantea A., Noonan D.M., Albini A., et al. (2002) The HtrA1 serine protease is down-regulated during human melanoma progression and represses growth of metastatic melanoma cells. Oncogene, 21, 6684–6688.
»Penn Text »CrossRef »Medline »Web of Science

22. Chien J., Staub J., Hu S.I., Erickson-Johnson M.R., Couch F.J., Smith D.I., Crowl R.M., Kaufmann S.H., Shridhar V. (2004) A candidate tumor suppressor HtrA1 is downregulated in ovarian cancer. Oncogene, 23, 1636–1644.
»Penn Text »CrossRef »Medline »Web of Science

23. De Luca A., De Falco M., Severino A., Campioni M., Santini D., Baldi F., Paggi M.G., Baldi A. (2003) Distribution of the serine protease HtrA1 in normal human tissues. J. Histochem. Cytochem., 51, 1279–1284.
»Abstract/FREE Full Text

24. Bowden M.A., Di Nezza-Cossens L.A., Jobling T., Salamonsen L.A., Nie G. (2006) Serine proteases HTRA1 and HTRA3 are down-regulated with increasing grades of human endometrial cancer. Gynecol. Oncol., 103, 253–260.
»Penn Text »CrossRef »Medline »Web of Science

25. Mullany S.A., Moslemi-Kebria M., Rattan R., Khurana A., Clayton A., Ota T., Mariani A., Podratz K.C., Chien J., Shridhar V. (2011) Expression and functional significance of HtrA1 loss in endometrial cancer. Clin. Cancer Res., 17, 427–436.
»Abstract/FREE Full Text

26. Shridhar V., Sen A., Chien J., Staub J., Avula R., Kovats S., Lee J., Lillie J., Smith D.I. (2002) Identification of underexpressed genes in early- and late-stage primary ovarian tumors by suppression subtraction hybridization. Cancer Res., 62, 262–270.
»Abstract/FREE Full Text

27. Wang N., Eckert K.A., Zomorrodi A.R., Xin P., Pan W., Shearer D.A., Weisz J., Maranus C.D., Clawson G.A. (2012) Down-regulation of HtrA1 activates the epithelial-mesenchymal transition and ATM DNA damage response pathways. PloS one, 7, e39446.
»Penn Text »CrossRef »Medline

28. Bianchi S., Di Palma G., Callus G.N., Taglia I., Poggiani A., Rosini F., Rufa A., Muresanu D.F., Cerase A., Dotti M.T., et al. (2014) Two novel HTRA1 mutations in a European CARASIL patient. Neurology, 82, 898–900.

»Penn Text »CrossRef »Medline

29. Chen Y., He Z., Meng S., Li L., Yang H., Zhang X. (2013) A novel mutation of the high-temperature requirement A serine peptidase 1 (HTRA1) gene in a Chinese family with cerebral autosomal recessive arteriopathy with subcortical infarcts and leukoencephalopathy (CARASIL). J. Int. Med. Res., 41, 1445–1455.
»Abstract/FREE Full Text

30. Mendioroz M., Fernandez-Cadenas I., Del Rio-Espinola A., Rovira A., Sole F., Fernandez-Figueras M.T., Garcia-Patos V., Sastre-Garriga J., Domingues-Montanari S., Alvarez-Sabin J. et al. (2010) A missense HTRA1 mutation expands CARASIL syndrome to the Caucasian population. Neurology, 75, 2033–2035.
»Penn Text »CrossRef »Medline

31. Nishimoto Y., Shibata M., Nihonmatsu M., Nozaki H., Shiga A., Shirata A., Yamane K., Kosakai A., Takahashi K., Nishizawa M. et al. (2011) A novel mutation in the HTRA1 gene causes CARASIL without alopecia. Neurology, 76, 1353–1355.
»Penn Text »CrossRef »Medline

32. Wang Y.L., Li C.F., Guo H.W., Cao B.Z. (2012) A novel mutation in the HTRA1 gene identified in Chinese CARASIL pedigree. CNS Neurosci. Ther., 18, 867–869.
»Penn Text »CrossRef »Medline »Web of Science

33. Dewan A., Liu M., Hartman S., Zhang S.S., Liu D.T., Zhao C., Tam P.O., Chan W.M., Lam D.S., Snyder M. et al. (2006) HTRA1 promoter polymorphism in wet age-related macular degeneration. Science, 314, 989–992.
»Abstract/FREE Full Text

34. Fritsche L.G., Chen W., Schu M., Yaspan B.L., Yu Y., Thorleifsson G., Zack D.J., Arakawa S., Cipriani V., Ripke S. et al. (2013) Seven new loci associated with age-related macular degeneration. Nat. Genet., 45, 433–439.
»Penn Text »CrossRef »Medline

35. Deangelis M.M., Ji F., Adams S., Morrison M.A., Harring A.J., Sweeney M.O., Capone A., Jr., Miller J.W., Dryja T.P., Ott J. et al. (2008) Alleles in the HtrA serine peptidase 1 gene alter the risk of neovascular age-related macular degeneration. Ophthalmology, 115, 1209–1215.
»Penn Text »CrossRef »Medline »Web of Science

36. Fritsche L.G., Loenhardt T., Janssen A., Fisher S.A., Rivera A., Keilhauer C.N., Weber B.H. (2008) Age-related macular degeneration is associated with an unstable ARMS2 (LOC387715) mRNA. Nat. Genet., 40, 892–896.
»Penn Text »CrossRef »Medline »Web of Science

37. Tam P.O., Ng T.K., Liu D.T., Chan W.M., Chiang S.W., Chen L.J., DeWan A., Hoh J., Lam D.S., Pang C.P. (2008) HTRA1 variants in exudative age-related macular degeneration and interactions with smoking and CFH. Invest. Ophthalmol. Vis. Sci., 49, 2357–2365.
»Abstract/FREE Full Text

38. Baaske P., Wienken C.J., Reineck P., Duhr S., Braun D. (2010) Optical thermophoresis for quantifying the buffer dependence of aptamer binding. Angew. Chem. Int. Ed. Engl., 49, 2238–2241.
»Penn Text »CrossRef »Medline

39. Duhr S., Braun D. (2006) Why molecules move along a temperature gradient. Proc. Natl. Acad. Sci. USA, 103, 19678–19682.
»Abstract/FREE Full Text

40. Adams S.R., Campbell R.E., Gross L.A., Martin B.R., Walkup G.K., Yao Y., Llopis J., Tsien R.Y. (2002) New biarsenical ligands and tetracysteine motifs for protein labeling in vitro and in vivo: synthesis and biological applications. J. Am. Chem. Soc., 124, 6063–6076.
»Penn Text »CrossRef »Medline »Web of Science

41. Madani F., Lind J., Damberg P., Adams S.R., Tsien R.Y., Graslund A.O. (2009) Hairpin structure of a biarsenical-tetracysteine motif determined by NMR spectroscopy. J. Am. Chem. Soc., 131, 4613–4615.
»Penn Text »CrossRef »Medline

42. Kim M.S., Song J., Park C. (2009) Determining protein stability in cell lysates by pulse proteolysis and Western blotting. Protein Sci., 18, 1051–1059.
»Penn Text »CrossRef »Medline

43. Kimchi-Sarfaty C., Oh J.M., Kim I.W., Sauna Z.E., Calcagno A.M., Ambudkar S.V., Gottesman M.M. (2007) A “silent” polymorphism in the MDR1 gene changes

substrate specificity. Science, 315, 525–528.
»Abstract/FREE Full Text

44. Na Y.R., Park C. (2009) Investigating protein unfolding kinetics by pulse proteolysis. Protein Sci., 18, 268–276.
»Penn Text »CrossRef »Medline

45. Park C., Marqusee S. (2005) Pulse proteolysis: a simple method for quantitative determination of protein stability and ligand binding. Nat. Methods, 2, 207–212.
»Penn Text »CrossRef »Medline »Web of Science

46. Ruggiano A., Foresti O., Carvalho P. (2014) Quality control: ER-associated degradation: protein quality control and beyond. J. Cell. Biol., 204, 869–879.
»Abstract/FREE Full Text

47. Launay S., Maubert E., Lebeurrier N., Tennstaedt A., Campioni M., Docagne F., Gabriel C., Dauphinot L., Potier M.C., Ehrmann M., et al. (2008) HtrA1-dependent proteolysis of TGF-beta controls both neuronal maturation and developmental survival. Cell Death Differ., 15, 1408–1416.
»Penn Text »CrossRef »Medline »Web of Science

48. Karring H., Poulsen E.T., Runager K., Thogersen I.B., Klintworth G.K., Hoirup P., Enghild J.J. (2013) Serine protease HtrA1 accumulates in corneal transforming growth factor beta induced protein (TGFBIp) amyloid deposits. Mol. Vis., 19, 861–876.
»Penn Text »Medline

49. Abe M., Harpel J.G., Metz C.N., Nunes I., Loskutoff D.J., Rifkin D.B. (1994) An assay for transforming growth factor-beta using cells transfected with a plasminogen activator inhibitor-1 promoter-luciferase construct. Anal. Biochem., 216, 276–284.
»Penn Text »CrossRef »Medline »Web of Science

50. Butovsky O., Jedrychowski M.P., Moore C.S., Cialic R., Lanser A.J., Gabriely G., Koeglsperger T., Dake B., Wu P.M., Doykan C.E., et al. (2014) Identification of a unique TGF-beta-dependent molecular and functional signature in microglia. Nat. Neurosci., 17, 131–143.
»Penn Text »CrossRef »Medline

51. Li J.J., Lu J., Kaur C., Sivakumar V., Wu C.Y., Ling E.A. (2008) Effects of hypoxia on expression of transforming growth factor-beta1 and its receptors I and II in the amoeboid microglial cells and murine BV-2 cells. Neuroscience, 156, 662–672.
»Penn Text »CrossRef »Medline

52. Paglinawan R., Malipiero U., Schlapbach R., Frei K., Reith W., Fontana A. (2003) TGFbeta directs gene expression of activated microglia to an anti-inflammatory phenotype strongly focusing on chemokine genes and cell migratory genes. Glia, 44, 219–231.
»Penn Text »CrossRef »Medline »Web of Science

53. Suzumura A., Sawada M., Yamamoto H., Marunouchi T. (1993) Transforming growth factor-beta suppresses activation and proliferation of microglia in vitro. J. Immunol., 151, 2150–2158.
»Abstract

54. Javelaud D., Mauviel A. (2004) Mammalian transforming growth factor-betas: Smad signaling and physio-pathological roles. Int. J. Biochem. Cell. Biol., 36, 1161–1165.
»Penn Text »CrossRef »Medline »Web of Science

55. Javelaud D., Mauviel A. (2004) [Transforming growth factor-betas: smad signaling and roles in physiopathology]. Pathol. Biol. (Paris), 52, 50–54.
»Penn Text »CrossRef »Medline

56. Javelaud D., Mauviel A. (2005) Crosstalk mechanisms between the mitogen-activated protein kinase pathways and Smad signaling downstream of TGF-beta: implications for carcinogenesis. Oncogene, 24, 5742–5750.
»Penn Text »CrossRef »Medline »Web of Science

57. Spittau B., Bilka J., Steinfath E., Zoller T., Krieglstein K. (2015) TGFbeta1 increases microglia-mediated engulfment of apoptotic cells via upregulation of the milk fat globule-EGF factor 8. Glia, 63, 142–153.
»Penn Text »CrossRef »Medline

58. Cao H.J., Hogg M.G., Martino J.J., Smith T.J. (1995) Transforming growth factor-beta induces plasminogen activator inhibitor type-1 in cultured human orbital fibroblasts. Invest. Ophthalmol. Vis. Sci., 36, 1411–1419.
»Abstract/FREE Full Text

59. Dong C., Zhu S., Wang T., Yoon W., Goldschmidt-Clermont P.J. (2002) Upregulation of PAI-1 is mediated through TGF-beta/Smad pathway in transplant arteriopathy. J. Heart Lung Transplant., 21, 999-1008.
»Penn Text »CrossRef »Medline »Web of Science

60. Kutz S.M., Hordines J., McKeown-Longo P.J., Higgins P.J. (2001) TGF-beta1-induced PAI-1 gene expression requires MEK activity and cell-to-substrate adhesion. J. Cell. Sci., 114, 3905-3914.
»Abstract/FREE Full Text

61. Hunt R.C., Simhadri V.L., Iandoli M., Sauna Z.E., Kimchi-Sarfaty C. (2014) Exposing synonymous mutations. Trends Genet., 30, 308-321.
»Penn Text »CrossRef »Medline »Web of Science

62. Brest P., Lapaquette P., Souidi M., Lebrigand K., Cesaro A., Vouret-Craviari V., Mari B., Barbry P., Mosnier J.F., Hebuterne X., et al. (2011) A synonymous variant in IRGM alters a binding site for miR-196 and causes deregulation of IRGM-dependent xenophagy in Crohn's disease. Nat. Genet., 43, 242-245.
»Penn Text »CrossRef »Medline

63. Chamary J.V., Hurst L.D. (2005) Evidence for selection on synonymous mutations affecting stability of mRNA secondary structure in mammals. Genome Biol., 6, R75.
»Penn Text »CrossRef »Medline

64. Chamary J.V., Hurst L.D. (2009) The price of silent mutations. Sci. Am., 300, 46-53.
»Penn Text »Medline »Web of Science

65. Chamary J.V., Parmley J.L., Hurst L.D. (2006) Hearing silence: non-neutral evolution at synonymous sites in mammals. Nat. Rev. Genet., 7, 98-108.
»Penn Text »CrossRef »Medline »Web of Science

66. Duan J., Antezana M.A. (2003) Mammalian mutation pressure, synonymous codon choice, and mRNA degradation. J. Mol. Evol., 57, 694-701.
»Penn Text »CrossRef »Medline »Web of Science

67. Duan J., Wainwright M.S., Comeron J.M., Saitou N., Sanders A.R., Gelernter J., Gejman P.V. (2003) Synonymous mutations in the human dopamine receptor D2 (DRD2) affect mRNA stability and synthesis of the receptor. Hum. Mol. Genet., 12, 205-216.
»Abstract/FREE Full Text

68. Lampson B.L., Pershing N.L., Prinz J.A., Lacsina J.R., Marzluff W.F., Nicchitta C.V., MacAlpine D.M., Counter C.M. (2013) Rare codons regulate KRas oncogenesis. Curr. Biol., 23, 70-75.
»Penn Text »CrossRef »Medline

69. Nackley A.G., Shabalina S.A., Tchivileva I.E., Satterfield K., Korchynskyi O., Makarov S.S., Maixner W., Diatchenko L. (2006) Human catechol-O-methyltransferase haplotypes modulate protein expression by altering mRNA secondary structure. Science, 314, 1930-1933.
»Abstract/FREE Full Text

70. Zhang F., Saha S., Shabalina S.A., Kashina A. (2010) Differential arginylation of actin isoforms is regulated by coding sequence-dependent degradation. Science, 329, 1534-1537.
»Abstract/FREE Full Text

71. Fung K.L., Pan J., Ohnuma S., Lund P.E., Pixley J.N., Kimchi-Sarfaty C., Ambudkar S.V., Gottesman M.M. (2014) MDR1 synonymous polymorphisms alter transporter specificity and protein stability in a stable epithelial monolayer. Cancer Res., 74, 598-608.
»Abstract/FREE Full Text

72. Vorwerk P., Hohmann B., Oh Y., Rosenfeld R.G., Shymko R.M. (2002) Binding properties of insulin-like growth factor binding protein-3 (IGFBP-3), IGFBP-3 N- and C-terminal fragments, and structurally related proteins mac25 and connective tissue growth factor measured using a biosensor. Endocrinology, 143, 1677-1685.
»Penn Text »CrossRef »Medline »Web of Science

73. Dickey S.W., Baker R.P., Cho S., Urban S. (2013) Proteolysis inside the membrane is a rate-governed reaction not driven by substrate affinity. Cell, 155, 1270-1281.
»Penn Text »CrossRef »Medline

74. Bai Y., Liang S., Yu W., Zhao M., Huang L., Zhao M., Li X. (2014) Semaphorin 3A blocks the formation of pathologic choroidal neovascularization induced by transforming growth factor beta. Mol. Vis., 20, 1258-1270.

»Penn Text »Medline

75. Guymer R.H., Tao L.W., Goh L.K., Liew D., Ischenko O., Rohman L.D., Aung K., Cipriani T., Cain M., Richardson A.J. et al. (2011) Identification of urinary biomarkers for age-related macular degeneration. Invest. Ophthalmol. Vis. Sci., 52, 4639–4644.
»Abstract/FREE Full Text

76. Lyzogubov V.V., Tytarenko R.G., Liu J., Bora N.S., Bora P.S. (2011) Polyethylene glycol (PEG)-induced mouse model of choroidal neovascularization. J. Biol. Chem., 286, 16229–16237.
»Abstract/FREE Full Text

77. Promsote W., Veeranan-Karmegam R., Ananth S., Shen D., Chan C.C., Lambert N.A., Ganapathy V., Martin P.M. (2014) L-2-oxothiazolidine-4-carboxylic acid attenuates oxidative stress and inflammation in retinal pigment epithelium. Mol. Vis., 20, 73–88.
»Penn Text »Medline

78. Vidro-Kotchan E., Yendluri B.B., Le-Thai T., Tsin A. (2011) NBHA reduces acrolein-induced changes in ARPE-19 cells: possible involvement of TGFbeta. Curr. Eye Res., 36, 370–378.
»Penn Text »CrossRef »Medline »Web of Science

79. Yu A.L., Fuchshofer R., Kook D., Kampik A., Bloemendal H., Welge-Lussen U. (2009) Subtoxic oxidative stress induces senescence in retinal pigment epithelial cells via TGF-beta release. Invest. Ophthalmol. Vis. Sci., 50, 926–935.
»Abstract/FREE Full Text

80. Yu A.L., Lorenz R.J., Haritoglou C., Kampik A., Welge-Lussen U. (2009) Biological effects of native and oxidized low-density lipoproteins in cultured human retinal pigment epithelial cells. Exp. Eye Res., 88, 495–503.
»Penn Text »CrossRef »Medline

81. Hughes V. (2012) Microglia: the constant gardeners. Nature, 485, 570–572.
»Penn Text »CrossRef »Medline »Web of Science

82. Kreutzberg G.W. (1996) Microglia: a sensor for pathological events in the CNS. Trends Neurosci., 19, 312–318.
»Penn Text »CrossRef »Medline »Web of Science

83. Tambuyzer B.R., Ponsaerts P., Nouwen E.J. (2009) Microglia: gatekeepers of central nervous system immunology. J. Leukoc. Biol., 85, 352–370.
»Abstract/FREE Full Text

84. Schapansky J., Nardozzi J.D., LaVoie M.J. (2015) The complex relationships between microglia, alpha-synuclein, and LRRK2 in Parkinson's disease. Neuroscience, 302, 74–88.
»Penn Text »CrossRef »Medline

85. Bamberger M.E., Landreth G.E. (2002) Inflammation, apoptosis, and Alzheimer's disease. Neuroscientist, 8, 276–283.
»Abstract/FREE Full Text

86. D'Andrea M.R., Cole G.M., Ard M.D. (2004) The microglial phagocytic role with specific plaque types in the Alzheimer disease brain. Neurobiol. Aging, 25, 675–683.
»Penn Text »CrossRef »Medline »Web of Science

87. Latta C.H., Brothers H.M., Wilcock D.M. (2015) Neuroinflammation in Alzheimer's disease; a source of heterogeneity and target for personalized therapy. Neuroscience, 302, 103–111.
»Penn Text »CrossRef »Medline

88. Lue L.F., Schmitz C., Walker D.G. (2015) What happens to microglial TREM2 in Alzheimer's disease: Immunoregulatory turned into immunopathogenic? Neuroscience, 302, 130–150.
»Penn Text

89. Streit W.J., Miller K.R., Lopes K.O., Njie E. (2008) Microglial degeneration in the aging brain--bad news for neurons? Front. Biosci., 13, 3423–3438.
»Penn Text »Medline

90. Langmann T. (2007) Microglia activation in retinal degeneration. J. Leukoc. Biol., 81, 1345–1351.
»Abstract/FREE Full Text

91. Ma W., Cojocaru R., Gotoh N., Gieser L., Villasmil R., Cogliati T., Swaroop A., Wong W.T. (2013) Gene expression changes in aging retinal microglia: relationship to microglial support functions and regulation of activation. Neurobiol. Aging, 34, 2310–2321.
»Penn Text »CrossRef »Medline

92. Ma W., Coon S., Zhao L., Fariss R.N., Wong W.T. (2013) A2E accumulation influences retinal microglial activation and complement regulation. Neurobiol. Aging, 34, 943–960.
»Penn Text »CrossRef »Medline »Web of Science

93. Wong W.T. (2013) Microglial aging in the healthy CNS: phenotypes, drivers, and rejuvenation. Front. Cell. Neurosci., 7, 22.
»Penn Text »Medline

94. Damani M.R., Zhao L., Fontainhas A.M., Amaral J., Fariss R.N., Wong W.T. (2011) Age-related alterations in the dynamic behavior of microglia. Aging Cell, 10, 263–276.
»Penn Text »CrossRef »Medline »Web of Science

95. Karlstetter M., Langmann T. (2014) Microglia in the aging retina. Adv. Exp. Med. Biol., 801, 207–212.
»Penn Text »CrossRef »Medline

96. Cekanaviciute E., Fathali N., Doyle K.P., Williams A.M., Han J., Buckwalter M.S. (2014) Astrocytic transforming growth factor-beta signaling reduces subacute neuroinflammation after stroke in mice. Glia, 62, 1227–1240.
»Penn Text »CrossRef »Medline

97. Huang W.C., Yen F.C., Shie F.S., Pan C.M., Shiao Y.J., Yang C.N., Huang F.L., Sung Y.J., Tsay H.J. (2010) TGF-beta1 blockade of microglial chemotaxis toward Abeta aggregates involves SMAD signaling and down-regulation of CCL5. J. Neuroinflammation, 7, 28.
»Penn Text »CrossRef »Medline

98. Norden D.M., Fenn A.M., Dugan A., Godbout J.P. (2014) TGFbeta produced by IL-10 redirected astrocytes attenuates microglial activation. Glia, 62, 881–895.
»Penn Text »CrossRef »Medline »Web of Science

99. Rozovsky I., Finch C.E., Morgan T.E. (1998) Age-related activation of microglia and astrocytes: in vitro studies show persistent phenotypes of aging, increased proliferation, and resistance to down-regulation. Neurobiol. Aging, 19, 97.
»Penn Text »CrossRef »Medline »Web of Science

100. Friedrich U., Myers C.A., Fritsche L.G., Milenkovich A., Wolf A., Corbo J.C., Weber B.H. (2011) Risk- and non-risk-associated variants at the 10q26 AMD locus influence ARMS2 mRNA expression but exclude pathogenic effects due to protein deficiency. Hum. Mol. Genet., 20, 1387–1399.
»Abstract/FREE Full Text

101. Genomes Project CAbecasis G.R., Auton A., Brooks L.D., DePristo M.A., Durbin R.M., Handsaker R.E., Kang H.M., Marth G.T., McVean G.A. (2012) An integrated map of genetic variation from 1,092 human genomes. Nature, 491, 56–65.
»Penn Text »CrossRef »Medline »Web of Science

102. Grassmann F., Friedrich U., Fauser S., Schick T., Milenkovic A., Schulz H.L., von Strachwitz C.N., Rettenbacher T., Lichtner P., Meitinger T., et al. (2015) A candidate gene association study identifies DAPL1 as a female-specific susceptibility locus for age-related macular degeneration (AMD). Neuromolecular Med., 17, 111–120.
»Penn Text »CrossRef »Medline

103. Team RDC. (2010) R: a language and environment for statistical computing. R Foundation for Statistical Computing.

104. Ebert S., Weigelt K., Walczak Y., Drobnik W., Mauerer R., Hume D.A., Weber B.H., Langmann T. (2009) Docosahexaenoic acid attenuates microglial activation and delays early retinal degeneration. J. Neurochem., 110, 1863–1875.
»Penn Text »CrossRef »Medline »Web of Science

105. Laemmli U.K. (1970) Cleavage of structural proteins during the assembly of the head of bacteriophage T4. Nature, 227, 680–685.
»Penn Text »CrossRef »Medline »Web of Science

106. Karlstetter M., Walczak Y., Weigelt K., Ebert S., Van den Brulle J., Schwer H., Fuchshofer R., Langmann T. (2010) The novel activated microglia/macrophage WAP

domain protein, AMWAP, acts as a counter-regulator of proinflammatory response. J. Immunol., 185, 3379–3390.
» Abstract/FREE Full Text

Articles citing this article

Vitamin A-aldehyde adducts: AMD risk and targeted therapeutics
Proc. Natl. Acad. Sci. USA (2016) 0 (2016): 1600474113v1-201600474
» Abstract » Full Text (PDF)

Online ISSN 1460-2083 - Print ISSN 0964-6906